Research Article

For reprint orders, please contact: reprints@futuremedicine.com

Regenerative Medicine

Bilayered vascular graft derived from human induced pluripotent stem cells with biomimetic structure and function

Background: We developed an aligned bi-layered vascular graft derived from human induced pluripotent stem cells (iPSCs) that recapitulates the cellular composition, orientation, and anti-inflammatory function of blood vessels. **Materials & methods:** The luminal layer consisted of longitudinal-aligned nanofibrillar collagen containing primary endothelial cells (ECs) or iPSC-derived ECs (iPSC-ECs). The outer layer contained circumferentially oriented nanofibrillar collagen with primary smooth muscle cells (SMCs) or iPSC-derived SMCs(iPSC-SMCs). **Results:** On the aligned scaffolds, cells organized F-actin assembly within 8° from the direction of nanofibrils. When compared to randomly-oriented scaffolds, EC-seeded aligned scaffolds had significant reduced inflammatory response, based on adhesivity to monocytes. **Conclusion:** This study highlights the importance of anisotropic scaffolds in directing cell form and function, and has therapeutic significance as physiologically relevant blood vessels.

Keywords: collagen • endothelial • extracellular matrix • iPSC • nanofibrillar • scaffolds • smooth muscle • stem cells • tissue engineering • vascular graft

Karina H Nakayama[‡,1,2,3], Prajakta A Joshi[‡,3,4], Edwina S Lai[5], Prachi Gujar[6], Lydia-M Joubert[7], Bertha Chen[6] & Ngan F Huang*[,1,2,3]

[1]Stanford Cardiovascular Institute, Stanford University, Stanford, CA 94305, USA
[2]Department of Cardiothoracic Surgery, Stanford University, 300 Pasteur Drive, Stanford, CA 94305-5407, USA
[3]Veterans Affairs Palo Alto Health Care System, Palo Alto, CA 94304, USA
[4]Department of Biological Sciences, San Jose State University, San Jose, CA 95112, USA
[5]Department of Chemical Engineering, Stanford University, Stanford, CA 94305, USA
[6]Department of Obstetrics & Gynecology, Stanford University, Stanford, CA 94305, USA
[7]Cell Sciences Imaging Facility, Stanford University, Stanford, CA 94305, USA
*Author for correspondence:
Tel.: +1 650 849 0559
Fax: +1 650 725 3846
ngantina@stanford.edu
‡Authors contributed equally

Background

Over 24 million people in the USA suffer from coronary heart disease, stroke or peripheral arterial disease as a result of atherosclerotic lesion formation [1]. The current standard of care to treat patients in need of conduit vessels and bypass grafts is the use of an autologous donor vessel. Over one million vascular reconstructive surgeries are performed annually in the USA [2]. However, greater than 50% of vascular grafts placed in the lower extremities fail within the first 10 years [3], due to progressive intimal narrowing leading to hyperplasia. Additionally, damage to the delicate endothelium during vascular invention causes recruitment of monocytes, which can give rise to neointimal hyperplasia [4]. Availability of healthy and suitable autologous vessels is often limited in this patient population in part due to existing endothelial dysfunction. Although commercial polymeric bypass grafts are a suitable alternative for patients who lack suitable donor vessels, they do not support long-term patency as a small-diameter vascular graft [5,6]. Therefore, there is a growing demand to develop cell-based small-diameter vascular grafts that resist thrombosis and support graft patency.

The goal of vascular tissue engineering is to mimic the native blood vessel, which is composed of endothelial cells (ECs) that line the inner lumen, surrounded by a circumferential layer of smooth muscle cells (SMCs). Within blood vessels, the ECs that line the intimal layer are known to play an important functional role in resisting atherogenesis by inhibiting adhesion of lipogenic proteins and monocytes in the circulating blood [7]. In tissue-engineered vascular grafts, an endothelialized lumen has been shown to mediate thrombosis [8]; however, the mechanical integrity of these vascular scaffolds is suboptimal, possibly due to a lack of mature SMCs [9]. In addition to improved mechanical integrity, addition of SMCs has been shown to regulate EC function by increasing expression of angiogenic factors [10].

Future Medicine part of fsg

In addition to the cellular composition, the native blood vessel is composed of fibrillar extracellular matrices (ECMs) at the nano- and micro-scale [11]. In the straight segments of blood vessels, which are generally resistant to atherosclerotic lesion formation, the ECs are oriented along the direction of blood flow. In these atheroprotective regions, the ECs are nonimmunogenic and secrete high levels of vasoprotective factors. In contrast, in the bends and bifurcations of blood vessels, which are prone to atherosclerotic lesion formation, the ECs are randomly oriented in morphology, while functionally they have elevated platelet and leukocyte adhesion and infiltration. Increasing evidence suggests that EC morphology may be associated with atheroprotective function [12,13].

In this work, we employed nanopatterning cues composed of collagen to direct cellular orientation and function of human ECs and SMCs derived from human induced pluripotent stem cells (iPSC-ECs, iPSC-SMCs), which serve as an unlimited source of autologous therapeutic cells. While others have fabricated single and bilayer vascular grafts using cell sheets [14] or decellularized tissues [15], we propose a facile approach to generate a physiologically aligned bilayer nanofibrillar graft by taking advantage of the pH dependency of collagen fibrillogenesis [12,16]. Purified collagen type I, which is an ECM that is abundant in biological tissues, persists in monomeric form at low pH, but once neutralized it rapidly undergoes a fibrillogenesis process to create triple helical fibrils. Extrusion of the acidic collagen monomers into a pH neutral buffer in the presence of shear enables the collagen fibrils to preferentially organize in the direction of the extrusion process to create aligned nanofibrils without the need of sophisticated equipment.

The overall aim of this work was to generate a biomimetic vascular graft with physiological cellular orientation that is functionally anti-inflammatory. Our primary hypothesis was that the aligned bilayered vascular graft will direct cellular organization of the iPSC-ECs and iPSC-SMCs along their physiological orientations and exert anti-inflammatory function as a measure of atheroprotection.

Materials & methods

Generation of aligned bilayered nanofibrillar collagen graft

An aligned bilayered vascular graft was generated by first creating a hollow cylindrical conduit composed of longitudinally oriented nanofibrils, followed by wrapping of aligned solid strips to form the outer circumferential layer. The hollow longitudinal inner layer was fabricated by extruding high concentration rat tail collagen type I (30 mg/ml, BD Biosciences) from a custom aluminum syringe with a centrally located mandrel (1 mm diameter) at a rate of approximately 3 ml/min and a velocity of approximately 300 mm/s directly in warm pH neutral 10× phosphate-buffered saline (PBS) to initiate immediate fibrillogenesis [12,16], as shown in Figure 1A. To create the circumferential outer layer, strips of parallel-aligned collagen were fabricated by extruding collagen from a 22G blunt tip needle at the same speed into warm pH neutral buffer to initiate immediate fibrillogenesis (Figure 1B). After drying of the single-layered conduit and strips separately for 16 h, the strips were wrapped in a circumferential direction along the length of the single-layered conduit (Figure 1B) to create the bilayered graft. Extrusion of monomeric collagen at a low speed (~0.3 ml/min) was used to generate randomly oriented nanofibrillar collagen strips or conduits.

Culture of primary cells on the collagen grafts

For cell culture studies, the nanofibrillar collagen scaffolds were sterilized in 70% ethanol and rehydrated in PBS. The collagen scaffolds were seeded with either primary human dermal microvascular ECs (HMDECs, Lonza, passage 7–10) in EGM-2MV growth media (Lonza) or primary human aortic vascular SMCs (Life Technologies, passage 6–10) in Medium 231 with smooth muscle growth supplement (SMGM, Life Technologies). ECs and SMCs were seeded at 125,000 cells/cm^2 and cultured in a 1:1 ratio of endothelial growth media (EGM-2MV) media to Medium 231 with SMGM (Life Technologies) at 37°C and 5% CO_2. Bilayered grafts were seeded first with SMCs that were allowed to attach to the outer layer, with nylon tubing placed in the lumen of the graft to prevent cell adhesion to the intimal layer. After incubation for 16 h, the tubing was then removed and HMDECs were seeded into the inner lumen using a 20G syringe.

Culture of iPSC-derived cell types on the collagen grafts

The human iPSC-ECs were generated from the HUF5 iPSC line whose generation and characterization was previously described [17]. The HUF5 iPSC line was generally from healthy adult human fibroblasts retrovirally transduced by *Oct3/4*, *Sox2*, *KLF4* and *c-myc* transgenes. Briefly, the iPSCs were differentiated from embryoid body outgrowths in an inducing media containing VEGF (50 ng/ml) and BMP4 (50 ng/ml). Two weeks after the onset of differentiation, approximately 20% of cells expressed the endothelial marker VE-cadherin, based on FACS. The iPSC-ECs were expanded in EGM-2MV and express known EC markers, including CD31, VE-cadherin and endothelial nitric oxide synthase (eNOS) [18]. Furthermore, the cells form tube-like structures in matrigel and take up

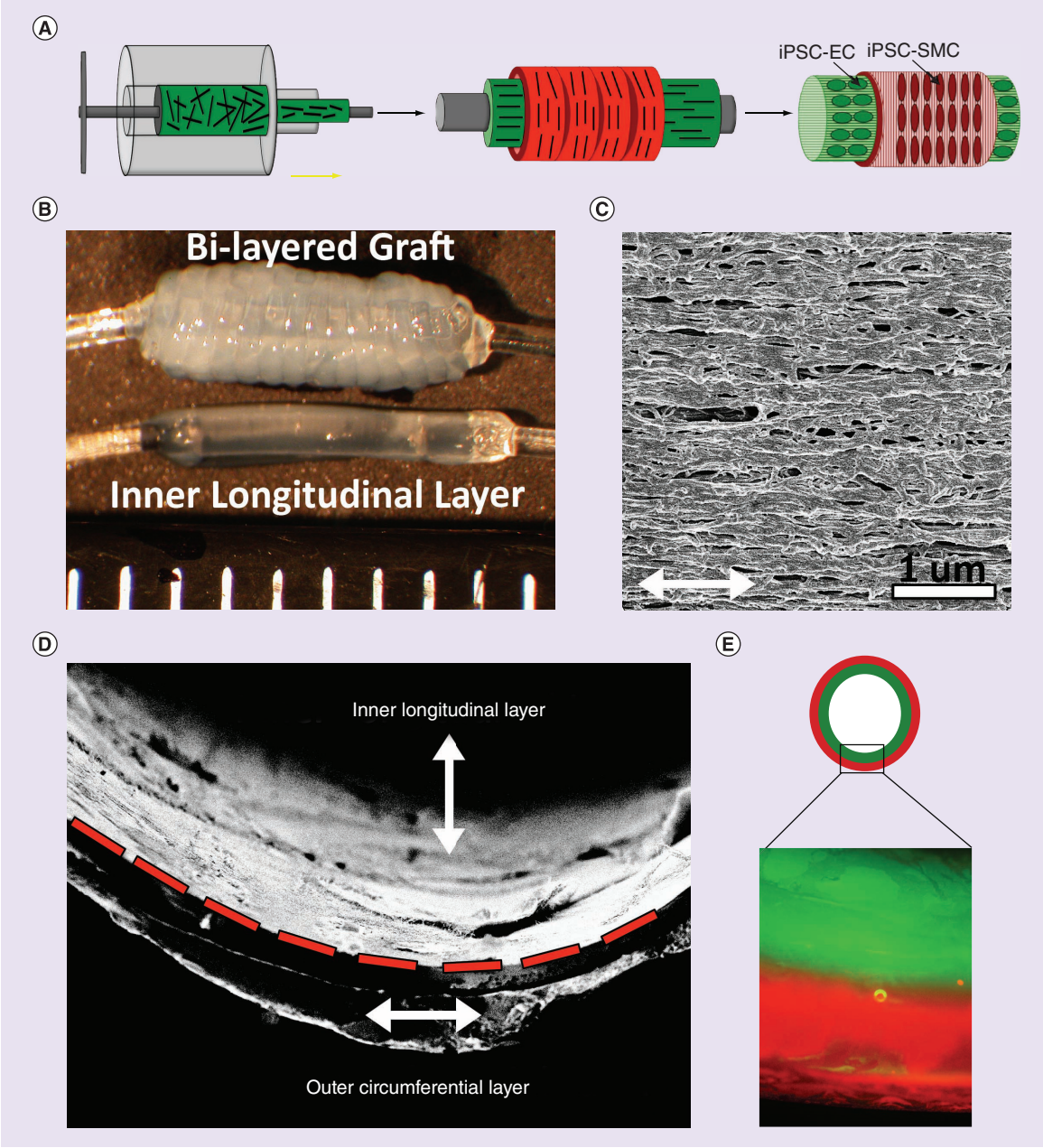

Figure 1. Production of a bilayered aligned nanofibrillar collagen graft. Schematic of the bilayered graft fabrication showing extrusion of collagen using concentric mandrels to aligned collagen fibrils in the longitudinal direction to create the inner hollow graft. The longitudinally aligned inner layer is circumferentially wrapped with an outer layer of aligned collagen. **(A)** The cellularized vascular graft has an inner layer of longitudinally oriented endothelial cells and an outer layer of circumferentially oriented smooth muscle cells. **(B)** The inner longitudinal layer alone (bottom) and the complete bilayered graft are supported by Nylon tubing before drying. Each tick represents 1 mm. Scanning electron microscopy image shows the organization of aligned collagen fibrils. Scale bar = 1 μm. **(C)** Arrow depicts direction of fibrils. Scanning electron microscopy depicts transverse section of the bilayered graft. **(D)** Arrow depicts direction of fibrils, and dotted line marks the interface between the two layers. **(E)** Fluorescently labeled inner layer (green) and outer layer (red) of the bilayered graft provide increased visualization of the two layers.
EC: Endothelial cell; iPSC: Induced pluripotent stem cell; SMC: Smooth muscle cell.
For color images please see online at www.futuremedicine.com/doi/full/10.2217/RME.15.45

acetylated low-density lipoprotein (LDL), which are both functional characteristics of ECs [18].

For smooth muscle differentiation, iPSCs were differentiated in a monolayer setting using the same induc-

ing media as was used for endothelial differentiation. After 8 days, the cells were FACS-purified for vascular progenitors that coexpressed CD31 and CD34. These vascular progenitors were induced toward smooth muscle lineage in SMGM on collagen IV (2.5 μg/cm^2)-coated dishes for three passages. iPSC-SMCs were spindle-like in morphology and expressed known smooth muscle markers, including SM22α, calponin, αSMA and desmin. These iPSC-SMCs resembled the phenotype of primary human aortic SMCs [19].

The collagen scaffolds were seeded with either hPSC-EC (passage 7–10) and/or iPSC-SMCs (passage 3–4) as described with the primary cells above. The iPSC-ECs and iPSC-SMCs were seeded onto the bilayered vascular grafts or strips at the same conditions as the primary ECs and SMCs (Figure 1B).

Scanning electron microscopy

For scanning electron microscopy (SEM) analysis, samples were fixed for 24 h with 4% paraformaldehyde and 2% glutaraldehyde in 0.1 M sodium cacodylate buffer (pH 7.2), rinsed in the same buffer and postfixed for 1 h with 1% aqueous OsO_4. After dehydration in an ascending ethanol series (50, 70, 90, 100% [twice]; 10 min each), samples were critical point dried with liquid CO_2 in a Tousimis Autosamdri-815B apparatus (Tousimis, MD, USA), mounted onto double-sided copper tape on 15 mm aluminum stubs (Electron Microscopy Sciences, PA, USA) and sputter-coated with 50 Å of gold–palladium using a Denton Desk II Sputter Coater (Denton Vacuum, NJ, USA). For cross-sectional views, samples were cut with a single-edge razor blade, and mounted onto low profile 45°/90° SEM stubs (Ted Pella, CA, USA) before sputter-coating. Visualization was performed with a Zeiss Sigma FESEM (Carl Zeiss Microscopy, NY, USA) operated at 2–3 kV, using InLens SE detection at working distance 4–5 mm. Images were captured in TIFF using store resolution 2048 × 1536 and a line averaging noise reduction algorithm.

Immunofluorescence staining

To visualize the two layers of the graft, the inner longitudinal layer was incubated with AlexaFluor 488 and the outer circumferential layer was incubated with AlexaFluor 594 (Life Technologies) and then imaged with fluorescence microscopy. To assess cell alignment, samples were stained for F-actin using fluorescently labeled phalloidin (Life Technologies). Cells on collagen scaffolds were stained fixed in 4% paraformaldehyde, permeabilized for 15 min with 0.5% Triton X-100 (Sigma), blocked with 1% bovine serum albumin for 1 h, followed by incubation with phalloidin-488 (Life Technologies) for 16 h. Samples were then counterstained with Hoechst33342 to visualize nuclei and imaged in the hydrated state in PBS.

Endothelial phenotypic marker expression in iPSC-ECs was confirmed by CD31 (Dako) expression. Similarly, smooth muscle marker, αSMA (Sigma) was used to verify smooth muscle phenotype. The staining procedure consisted of the same fixation, permeabilization and blocking steps as described above. After incubation with the primary antibody, the samples were incubated with corresponding Alexfluor fluorescently labeled secondary antibody.

Quantification of cellular alignment

Cell alignment was assessed by quantification of F-actin organization using Image J. The angle of orientation was defined as the angle formed by the cell's principal axis, relative to the direction of the collagen nanofibrils. A minimum angle of 0° denoted parallel alignment from the axis of the nanofibrils and a maximum of 90° suggested perpendicular alignment. Completely random orientation corresponded to an averaged angle of 45° based on an arbitrary axis. Phalloidin-labeled cells on randomly oriented and aligned collagen groups were imaged at 20× objectives. At least 60 cells were counted for each sample within each treatment group, and the angle values were averaged and reported as mean ± standard deviation (n = 3).

Monocyte adhesion assay

To assess the inflammatory effects of the longitudinally oriented ECs induced by the underlying aligned nanofribrillar scaffold, a monocyte adhesion assay was performed. Primary ECs or iPSC-ECs were seeded onto either aligned or randomly oriented collagen scaffolds and allowed to form a confluent cell monolayer to minimize the possibility of migration or exposure of underlying collagen. Cells were then treated with tissue necrosis factor alpha (TNF-α, 250 U/ml) in their corresponding growth media for 7 h. Afterward, two million human monocytes (U937, ATCC) were fluorescently labeled with 1 μM Cell Tracker™ Red CMPTX (Life Technologies) before incubating with the EC-seeded scaffolds at room temperature for 30 min in the presence of gentle agitation (20° z-axis setting on rocker). Unbound monocytes were washed away with PBS and the adherent monocytes were immediately imaged with a fluorescence microscope. To determine the specificity of monocyte adhesion to ECs, we performed additional experiments by replacing ECs with primary human fibroblasts (BJ, ATCC, passage 9–10).

For each sample, five fields were imaged at 10× objectives for each sample (primary ECs and iPSC-

ECs, n = 4; fibroblasts, n = 3). The number of adhered monocytes was counted and normalized to the area of the images. Monocytes at the edges of the collagen strips were excluded from analysis due to biased gravitational adherence in the grooves between the strips. The number of fluorescent monocytes per square micrometer was counted and graphical representation of data was reported as fold change relative to monocytes/mm^2 on ECs or iPSC-ECs on randomly oriented collagen.

Statistical analysis

Data are presented as mean ± standard deviation. Comparisons were conducted with an unpaired, two-tailed Student's t-test with unequal variances and significant differences defined by *$p < 0.05$.

Results

Generation of bilayered aligned nanofibrillar grafts

Bilayered grafts were generated using a high-velocity extrusion process to produce an aligned nanofibrillar hollow cylinder as the graft inner layer (Figure 1A) that was then wrapped circumferentially with aligned nanofibrillar collagen strips, forming an orthogonally oriented bilayered collagen scaffold (Figure 1B). The nanofibrillar orientation of collagen grafts was confirmed with SEM (Figure 1C), showing a longitudinally oriented inner layer, surrounded by a circumferentially oriented outer layer (Figure 1D). Individual nanofibrils were approximately 30 nm in diameter. To visualize the interface between the two layers, the inner longitudinal layer was stained with Alexafluor-488 and the outer circumferential layer was labeled with Alexafluor-594 secondary antibodies (Figure 1E).

Alignment of primary ECs & SMCs on aligned nanofibrillar grafts

Primary ECs and SMCs were seeded onto randomly oriented and aligned nanofibrillar collagen grafts to confluency. Staining for F-actin showed that cells became elongated and aligned along the direction of the collagen nanofibrils (Figure 2B & D), whereas on randomly oriented collagen the cells adopted a random distribution of orientations and a more cobblestone-like morphology (Figure 2A & C). Comparison of the relative angle of cell orientation revealed stark differences in alignment. The average angle for primary ECs on aligned nanofibrillar collagen was 8 ± 1°, in which the majority of the cells were angled at less than 10° (Figure 2E). In contrast, the average angle of alignment for randomly oriented primary ECs was 40 ± 3°, in which the angle of alignment distributed uniformly across a broad range of 0–90°. Alignment angles on aligned nanofibrillar scaffolds were significantly lower than those on randomly oriented scaffolds ($p < 0.001$). Similarly, primary SMCs aligned along the circumferential direction of the scaffold and had an average angle of alignment of 5 ± 1°, which was statistically significant when compared with the corresponding value of 37 ± 4° for SMCs on randomly oriented collagen scaffolds (Figure 2F; $p < 0.001$). Although the cells had well-developed actin cytoskeletal assembly, the cells did not appear to contract the random or aligned collagen scaffolds.

Alignment of iPSC-ECs & iPSC-SMCs on aligned nanofibrillar scaffolds

Toward clinical translation, we generated and cultured iPSC-ECs and iPSC-SMCs onto randomly oriented or aligned nanofibrillar collagen scaffolds for comparison of cellular alignment. Similar to the results from primary ECs, the iPSC-ECs demonstrated elongated morphology and preferential alignment along the direction of the collagen nanofibers on the aligned scaffolds (Figure 3C), whereas on randomly oriented collagen the cells adopted a random orientation and a more cobblestone-like morphology (Figure 3A). To verify their endothelial phenotype, the iPSC-ECs expressed the endothelial marker, CD31 (Figure 3B & D). Similar to that of primary ECs on aligned scaffolds, the iPSC-ECs had a statistically significant degree of alignment of 6 ± 1° on aligned scaffolds, when compared with a corresponding value of 39 ± 3° on randomly oriented scaffolds (Figure 3I; $p < 0.001$). These data demonstrate the similarity of iPSC-ECs to primary ECs in their organizational response to aligned nanopatterned scaffolds.

Like primary SMCs, iPSC-SMCs aligned circumferentially along the aligned nanofibrils, but were morphologically disorganized on the randomly oriented collagen (Figure 3E–H). The average angle of alignment for iPSC-SMCs on aligned nanofibrillar collagen was 4 ± 2°, compared with an average angle of 39 ± 5° for iPSC-SMCs on randomly oriented collagen scaffolds (Figure 3J) and was statistical significant between groups ($p < 0.001$). The iPSC-SMCs were shown to express the αSMA, demonstrating the ability of the cells to maintain their phenotype when cultured on the grafts (Figure 3F & H). Together, these data demonstrate the ability for aligned nanofibrillar scaffolds to modulate cellular elongation and alignment for both primary as well as iPSC-derived vascular lineages. Similar to the primary vascular cells, the iPSC-ECs and iPSC-SMCs did not appear to contract the random or aligned collagen scaffolds.

Monocyte adhesion to HMDEC & iPSC-EC

Development of atherosclerotic lesions is preceded by a chronic inflammatory response that includes increased

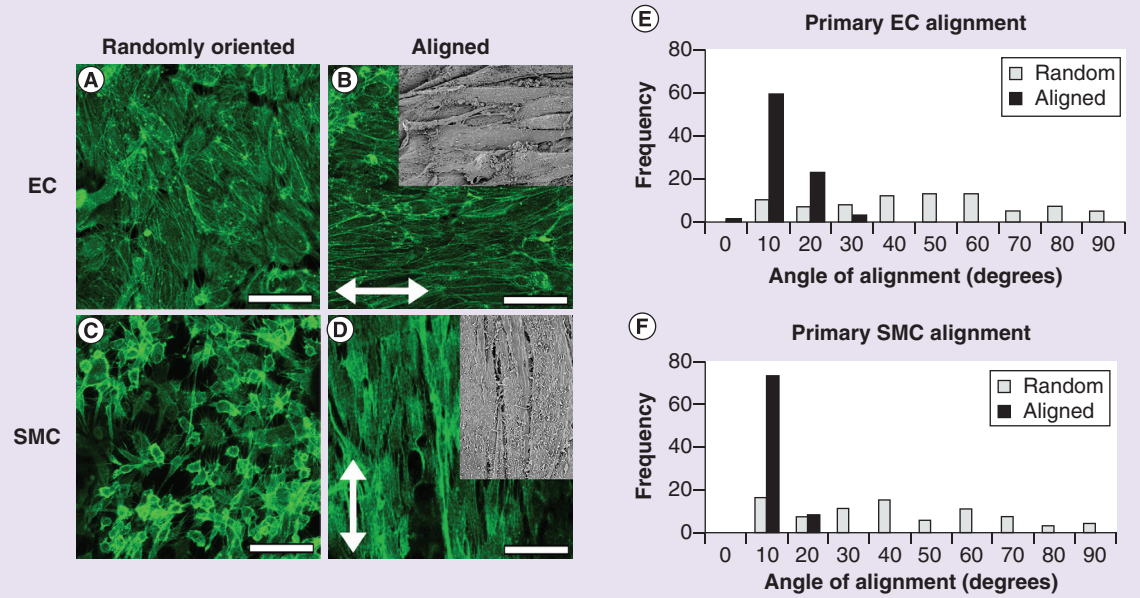

Figure 2. Primary endothelial cells and smooth muscle cells orient along the direction of collagen fibrils on aligned nanofibrillar graft. (A & B) F-actin staining of primary human endothelial cells, and **(C & D)** smooth muscle cells on randomly oriented or aligned nanofibrillar collagen scaffolds. Inset shows scanning electron microscopy of cells oriented along aligned fibril direction. Arrow depicts direction of fibrils. Scale bar = 50 μm. Quantification of cell angles on randomly oriented (white) versus aligned (black) collagen scaffolds for **(E)** endothelial cells and **(F)** smooth muscle cells.
EC: Endothelial cell; SMC: Smooth muscle cell.

adhesion of circulating monocytes to ECs lining the blood vessels. Given the importance of ECs in modulating anti-inflammatory properties within blood vessels, we sought to determine if the alignment of ECs had a functional benefit in mediating monocyte adhesion. Notably, the monocytes were 0.4 ± 0.2-fold less adherent to primary ECs when cultured on aligned nanofibrillar scaffolds than when compared with ECs randomly oriented scaffolds (Figure 4A, B & E). These results were also confirmed using iPSC-ECs, in which we observed a 0.6 ± 0.2-fold reduction in monocyte adhesion to iPSC-ECs when cultured on aligned nanofibrillar scaffolds, in comparison to randomly oriented scaffolds (Figure 4C, D & F). These results suggested that aligned nanofibrillar patterning may have therapeutic benefit in conferring anti-inflammatory properties to resist atherosclerotic lesion formation.

To assess whether the reduction in monocyte adhesion was EC specific, the assay was also performed using human fibroblasts instead of ECs. In comparison to monocyte adhesion onto ECs, monocyte adhesion onto fibroblasts was generally much reduced, and the level of monocyte adhesion was not statistically significant between the randomly oriented and aligned scaffolds. These data demonstrate that modulation of monocyte adhesion through cellular alignment is an endothelial-specific response.

Discussion

The salient findings of this study are that aligned nanofibrillar vascular grafts can: modulate the organization of both primary and iPSC-derived vascular lineages; and inhibit the inflammatory response of both primary ECs and iPSC-ECs. This work builds upon our previous generation of single-layered vascular grafts by creating a more physiologically relevant vascular graft composed of both intimal and medial layers [12]. Furthermore, the demonstrated similarities in morphology and inflammatory response between iPSC-derived vascular lineages and primary cells provide supporting evidence of iPSCs as a therapeutic cell source. These results have translational implications in the generation of iPSC-derived vascular grafts that resist inflammation, which may promote graft patency. Future directions consist of evaluating the patency of the bilayered vascular graft after interpositional grafting in a rodent model.

Limited suitability of autologous blood vessels and complications associated with commercially available synthetic grafts creates a growing demand for tissue-engineered alternatives for generating biomimetic vascular grafts. Approaches to constructing these engineered grafts have focused on providing the optimal microenvironment for growth of vascular cell types and tissue formation. One approach involves the use

of temperature-responsive substrates that allow the recovery of intact confluent cell sheets by controlling hydrophobicity states [20]. Using this technology, tissue-engineered blood vessels have been fabricated from multilayered smooth muscle, fibroblast and EC sheets [14] or combined with electrospun materials to generate bilayered vascular/SMC sheet scaffolds [21]. A notable advantage of the vascular grafts in the current study is the recapitulation of native cellular orientation, which is not easily achieved using cell sheet approaches. Scaffold nanostructure has been shown to play an integral role in modulating the phenotype, orientation and functional activity of ECs [22,23]. Although the scaffolds lack elastin, which confers elasticity in native vessels, it is likely that the vascular lineages would remodel the scaffold over time by secreting endogenous ECMs that may include elastin.

A common approach for producing nanofibrous scaffolds employs electrospinning technology, which utilizes a high voltage difference to spin micro- and even nanoscale fibers. Aligned nanofiber orientation can be accomplished with the use of either a rotating mandrel or through manipulation of the electric field that causes the fibers to alternate between two metal plates,

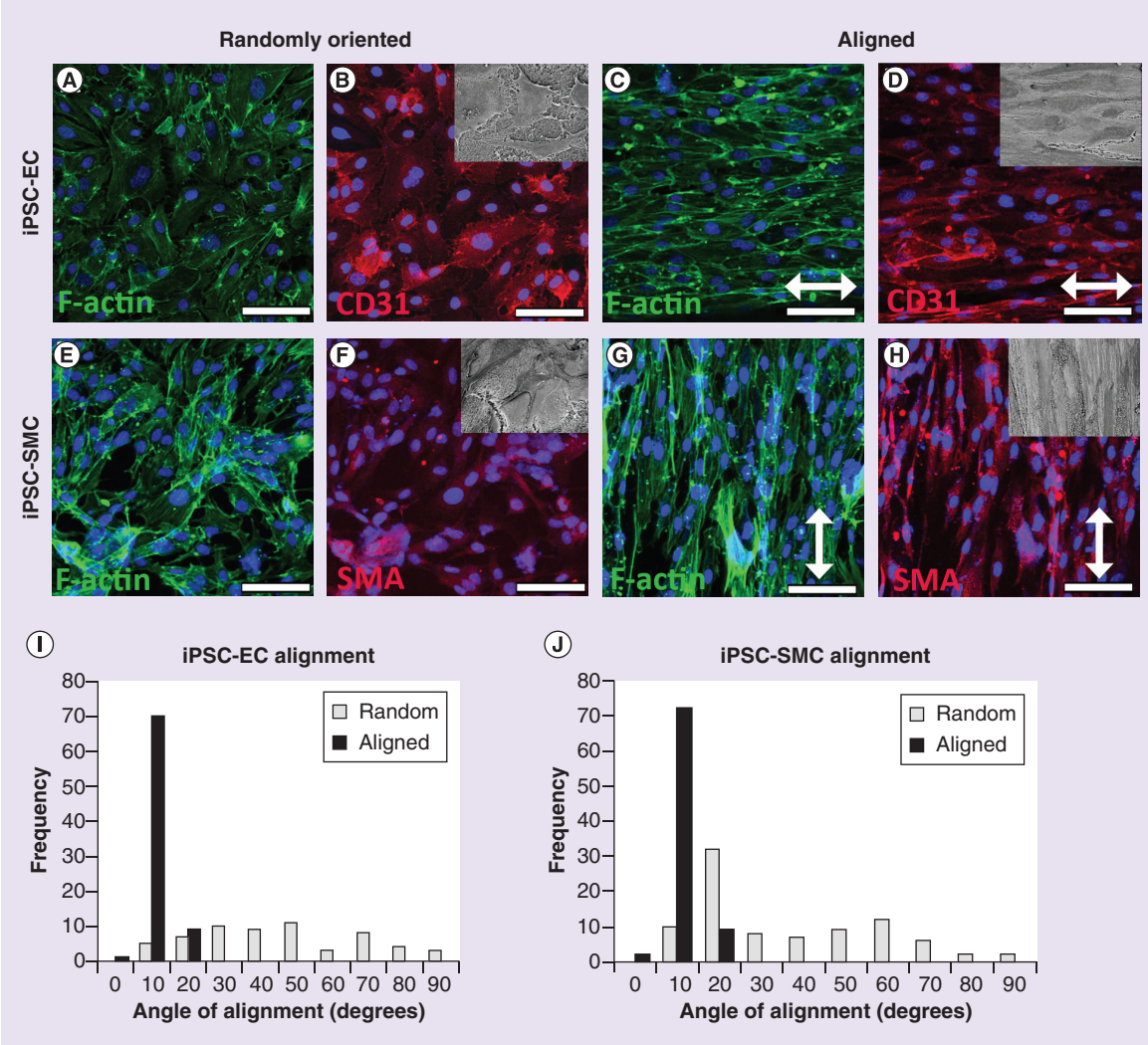

Figure 3. Human induced pluripotent stem cell-endothelial cells and induced pluripotent stem cell-smooth muscle cells orient along the direction of aligned nanofibrillar grafts. F-actin and CD31 staining of human induced pluripotent stem cell-endothelial cells **(A–D)** on **(A & B)** randomly oriented, or **(C & D)** aligned nanofibrillar collagen scaffolds. F-actin and αSMA staining of human induced pluripotent stem cell-smooth muscle cells on **(E & F)** randomly oriented, or **(G & H)** aligned nanofibrillar collagen scaffolds. Inset shows scanning electron microscopy of cells oriented along aligned fibril direction. Arrow depicts direction of fibrils. Scale bar = 50 μm. Quantification of cell orientation angles on randomly oriented (white) versus aligned (black) collagen scaffolds for **(I)** induced pluripotent stem cell-endothelial cells and **(J)** induced pluripotent stem cell-smooth muscle cells.
EC: Endothelial cell; iPSC: Induced pluripotent stem cell; SMC: Smooth muscle cell.

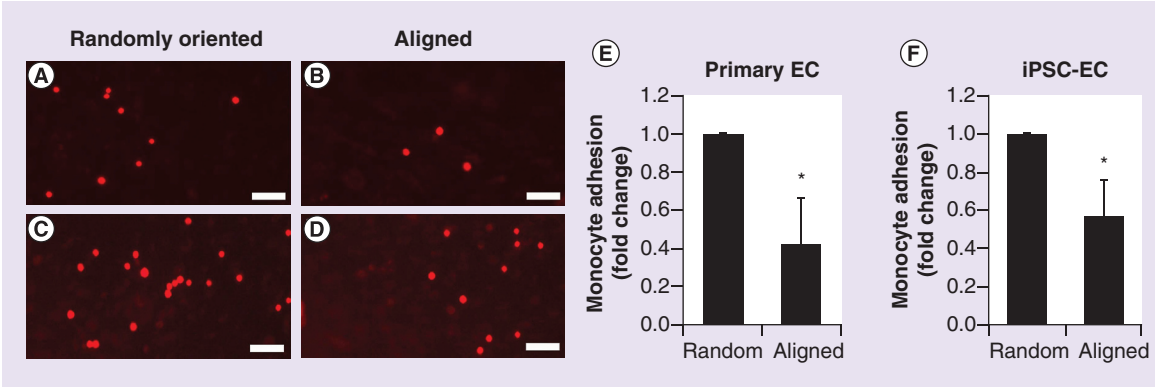

Figure 4. Adhesion of monocytes to primary endothelial cells and induced pluripotent stem cell-endothelial cells on aligned collagen graft. Representative image showing the relative degree of fluorescent monocytes adhered to the surface of activated primary endothelial cells (ECs) on **(A)** randomly oriented or **(B)** aligned collagen scaffolds. Representative image showing the relative degree of fluorescent monocytes adhered to the surface of activated induced pluripotent stem cell-ECs on **(C)** randomly oriented or **(D)** aligned collagen scaffolds. Relative levels of **(E)** monocyte adhesion on primary ECs or **(F)** induced pluripotent stem cell-ECs cultured on randomly oriented or aligned scaffolds.
Scale bar = 125 μm, *p < 0.05.
EC: Endothelial cell; iPSC: Induced pluripotent stem cell.

thereby creating oriented poly-ε-caprolactone (PCL) fibers either in the shape of large to medium diameter (25 mm diameter) and smaller diameter (<5 mm diameter) grafts, respectively [24,25]. Like electrospinning, our approach achieves a strong degree of nanoalignment of natural ECM fibers and, in addition, can create even smaller diameter vascular grafts (1 mm diameter). Additionally, our approach is facile in that it does not require specialized equipment or high voltages and can be fabricated using simple laboratory reagents. Recently, electrospun fibers encapsulating cells that form functional and viable 3D tissues have been demonstrated [26,27]. This has important implications in the development of aligned tissue-engineered constructs and presents a promising approach for creating aligned blood vessels.

To effectively recapitulate the architecture of the native blood vessel, many tissue-engineered grafts incorporate at least two layers: and inner layer of ECs that are a primary modulator of vessel health and an outer layer of SMCs that serve to provide tensile strength [9,28]. However, limited autologous sources of ECs and SMCs drive the development of patient-specific human iPSC-derived blood vessels. While tissue-engineered vascular grafts composed of either iPSC-SMCs [29,30] or iPSC-ECs [31] have been demonstrated, here we generate a vessel not only composed entirely of iPSC-derived vascular cell types but also induce physiologically relevant alignment of each cell type to produce a translatable biomimetic vascular graft. To our knowledge, this is the first report of a bilayered vascular graft with physiologically relevant cellular organization composed of iPSC-derived vascular lineages.

The development of atherosclerotic lesions and atherothrombosis involves a series of events, including increased expression of adhesion molecules (i.e., P-selectin, ICAM-1 and VCAM-1), inflammation, leukocyte recruitment and increased adhesion of platelets and monocytes [32]. We have shown that aligned nanofibrillar scaffolds induce EC alignment and reduce monocyte adhesion. However, future studies are needed to more extensively explore the contribution of anisotropic scaffolds to anti-inflammatory properties and to atherosclerosis.

Our finding that aligned nanofibrillar scaffolds induce alignment of primary and iPSC-derived vascular lineages suggest that the nanofibrillar scaffolds confer signaling cues that induce cellular reorganization. This phenomenon is in stark contrast to microscale cues such as microgrooves in which the cells are physically confined with limited degrees of freedom for cellular movement [33]. Our nanopatterned scaffolds do not physically restrain cell movement, so the resulting cellular reorganization is presumably induced by activation of mechanotransduction pathways. Integrins, which are transmembrane receptors that bind to ECMs, may likely be involved in the process, as they are also nanoscale in cluster size and have been shown to influence cell fate [34–36]. Further directions to elucidate the signaling mechanisms are warranted.

The current study is limited in the use of manually engineered scaffolds, which reduces the reproducibility of fabrication for preclinical and clinical testing. Automating the shear-mediated extrusion process using a syringe pump at defined velocities may further improve its reproducibility. Another limitation is the

integrity of the circumferential layer by wrapping of extruded strips around the luminal layer. Modifying the extrusion apparatus so as to extrude wide membranes may reduce the total number of strips needed to wrap around the luminal layer. The mechanical properties will need to be examined to ensure suitable physiological burst pressures before *in vivo* testing as an interpositional graft. Finally, a translational concern is the thrombogenicity of collagen when in direct contact with blood. Approaches to reduce thrombogenicity by conjugation of antithrombogenic compounds such as heparin [37] or hirudin [38] may improve the safety of the collagen scaffold from thrombosis.

Conclusion

This study utilizes nanotopographical cues to generate a nanofibrillar-aligned bilayered vascular graft composed of iPSC-ECs and iPSC-SMCs with physiologic orientation and atheroprotective function. This report is the first bioengineered bilayered vascular graft containing physiologically relevant cellular organization that is composed of iPSC-derived vascular lineages.

Future perspective

It is well established that cell shape, cytoskeletal reorganization and function are modulated by chemical and physical properties of an underlying substrate [39]. Future avenues of investigation include functional testing of the smooth muscle layer by pharmacologically induced vasoconstriction and elucidation of the cellular and molecular mechanisms underlying spatial nanopatterning-induced cellular effects. As the role of nanotopography in mediating cellular behavior and function becomes further elucidated, bioengineered nanoaligned 3D tissues may adopt a spatial patterning-based approach that preserves cellular alignment and function. This approach can be applied to any anisotropic tissue such as blood vessels, skeletal muscle and cardiac muscle. Moreover, as tissue engineering of vascular grafts moves toward clinical translation, use of autologous iPSCs as the cell source will be vital to ensure optimal host response and long-term viability and function. While there are numerous approaches to achieve micro- or nanoaligned substrates, an overriding theme in the next generation of engineered vascular grafts will be recapitulation of native cell orientation and function by signaling cues from the scaffold.

Acknowledgements

The authors acknowledge GG Fuller for useful discussion and technical advice.

Financial & competing interests disclosure

This study was supported in part by grants from the US NIH (R00HL098688 and EB020235-01 to NFH), Merit Review

Executive summary

Background

- Biomimetic tissue-engineered vascular grafts with physiological cellular composition, orientation and function are a promising approach for patients requiring coronary bypass grafting, peripheral artery bypass grafting or hemodialysis access.
- The purpose of this study was to develop a nanofibrillar-aligned bilayered vascular graft derived from human induced pluripotent stem cells (iPSCs) and to assess the effects of nanotopography on modulating cellular orientation and atheroprotective function.

Materials & methods

- A shear-mediated approach was used to generate aligned nanofibrillar collagen scaffolds.
- A bilayered vascular graft was composed of a longitudinally oriented luminal layer of endothelial cells (ECs) derived from primary cells or iPSCs (iPSC-ECs). The outer circumferentially oriented layer was composed of primary smooth muscle cells (SMCs) or those derived from iPSCs (iPSC-SMCs).
- Immunofluorescent staining for F-actin was used to quantify the angle of cellular alignment and adhesion of fluorescently labeled monocytes was used to assess atheroprotective function.

Results

- Primary human ECs and iPSC-ECs reorganized their actin cytoskeleton along the direction of the nanofibrils.
- Primary human SMCs and iPSC-SMCs became highly elongated and aligned their actin stress fiber assembly in the circumferential direction along the direction of the nanofibrils.
- Compared with cells grown on randomly oriented collagen scaffolds, the ECs and iPSC-ECs cultured on aligned nanofibrillar scaffolds had reduced adhesivity for monocytes.

Conclusion

- The current study highlights the importance of nanopatterning cues to direct cellular behavior and function.
- Generation of an iPSC-derived vascular graft that possesses physiologically relevant morphology and function holds substantial translational significance as a patient-specific biomimetic blood vessel that resists atherosclerotic lesion formation.

Award (1I01BX002310) from the Department of Veterans Affairs Biomedical Laboratory Research and Development to NF Huang, the Stanford Chemistry Engineering & Medicine for Human Health to NF Huang, the Stanford Cardiovascular Institute to NF Huang and the California Institute of Regenerative Medicine (CIRM Early Translational Research Award TR3-05569) to B Chen. KH Nakayama was supported by fellowships from the National Heart, Lung and Blood Institute (1T32HL098049) and the American Heart Association (15POST25560045). PA Joshi was supported by a fellowship from the San José State University Consortium for Stem Cell Internships in Laboratory-based Learning. The authors have no other relevant affiliations or financial involvement with any organization or entity with a financial interest in or financial conflict with the subject matter or materials discussed in the manuscript apart from those disclosed.

No writing assistance was utilized in the production of this manuscript.

References

Papers of special note have been highlighted as:
• of interest; •• of considerable interest

1 Writing Group M, Lloyd-Jones D, Adams RJ *et al.* Heart disease and stroke statistics – 2010 update: a report from the American Heart Association. *Circulation* 121(7), e46–e215 (2010).

2 Epstein AJ, Polsky D, Yang F, Yang L, Groeneveld PW. Coronary revascularization trends in the United States, 2001–2008. *JAMA* 305(17), 1769–1776 (2011).

3 Eslami MH, Gangadharan SP, Belkin M, Donaldson MC, Whittemore AD, Conte MS. Monocyte adhesion to human vein grafts: a marker for occult intraoperative injury? *J. Vasc. Surg.* 34(5), 923–929 (2001).

4 Rogers C, Welt FG, Karnovsky MJ, Edelman ER. Monocyte recruitment and neointimal hyperplasia in rabbits. Coupled inhibitory effects of heparin. *Arterioscler. Thromb. Vasc. Biol.* 16(10), 1312–1318 (1996).

5 Hasse B, Husmann L, Zinkernagel A, Weber R, Lachat M, Mayer D. Vascular graft infections. *Swiss Med. Wkly* 143, w13754 (2013).

6 Veith FJ, Gupta SK, Ascer E *et al.* Six-year prospective multicenter randomized comparison of autologous saphenous vein and expanded polytetrafluoroethylene grafts in infrainguinal arterial reconstructions. *J. Vasc. Surg.* 3(1), 104–114 (1986).

7 Cooke JP. Flow, no, and atherogenesis. *Proc. Natl Acad. Sci. USA* 100(3), 768–770 (2003).

•• **Describes the physiological relevance of vascular endothelial alignment with respect to flow, and the influence of cellular alignment on vascular inflammation.**

8 Melchiorri AJ, Hibino N, Fisher JP. Strategies and techniques to enhance the *in situ* endothelialization of small-diameter biodegradable polymeric vascular grafts. *Tissue Eng. Part B Rev.* 19(4), 292–307 (2013).

9 Neff LP, Tillman BW, Yazdani SK *et al.* Vascular smooth muscle enhances functionality of tissue-engineered blood vessels *in vivo*. *J. Vasc. Surg.* 53(2), 426–434 (2011).

10 Heydarkhan-Hagvall S, Helenius G, Johansson BR, Li JY, Mattsson E, Risberg B. Co-culture of endothelial cells and smooth muscle cells affects gene expression of angiogenic factors. *J. Cell Biochem.* 89(6), 1250–1259 (2003).

11 Stehbens WE, Martin BJ. Ultrastructural alterations of collagen fibrils in blood vessel walls. *Connect. Tissue Res.* 29(4), 319–331 (1993).

12 Lai ES, Huang NF, Cooke JP, Fuller GG. Aligned nanofibrillar collagen regulates endothelial organization and migration. *Regen. Med.* 7(5), 649–661 (2012).

•• **Examines how aligned nanofibrillar scaffolds influence primary endothelial cell organization and motility, with a focus on the role of the cytoskeleton in mediating the process.**

13 Vartanian KB, Berny MA, Mccarty OJ, Hanson SR, Hinds MT. Cytoskeletal structure regulates endothelial cell immunogenicity independent of fluid shear stress. *Am. J. Physiol. Cell Physiol.* 298(2), C333–C341 (2010).

14 L'heureux N, Germain L, Labbe R, Auger FA. *In vitro* construction of a human blood vessel from cultured vascular cells: a morphologic study. *J. Vasc. Surg.* 17(3), 499–509 (1993).

15 Hodde JP, Record RD, Tullius RS, Badylak SF. Retention of endothelial cell adherence to porcine-derived extracellular matrix after disinfection and sterilization. *Tissue Eng.* 8(2), 225–234 (2002).

16 Lai ES, Anderson CM, Fuller GG. Designing a tubular matrix of oriented collagen fibrils for tissue engineering. *Acta Biomater.* 7(6), 2448–2456 (2011).

17 Byrne JA, Nguyen HN, Reijo Pera RA. Enhanced generation of induced pluripotent stem cells from a subpopulation of human fibroblasts. *PLoS ONE* 4(9), e7118 (2009).

18 Rufaihah AJ, Huang NF, Jame S *et al.* Endothelial cells derived from human iPSCs increase capillary density and improve perfusion in a mouse model of peripheral arterial disease. *Arterioscler. Thromb. Vasc. Biol.* 31(11), e72–e79 (2011).

• **Describes the generation of endothelial cells from human induced pluripotent stem cells and the therapeutic application of these cells for the first time in a murine model of peripheral arterial disease.**

19 Marchand M, Anderson EK, Phadnis SM *et al.* Concurrent generation of functional smooth muscle and endothelial cells via a vascular progenitor. *Stem Cells Transl. Med.* 3(1), 91–97 (2014).

20 Nagase K, Kobayashi J, Okano T. Temperature-responsive intelligent interfaces for biomolecular separation and cell sheet engineering. *J. R. Soc. Interface* 6(Suppl. 3), S293–S309 (2009).

21 Ahn H, Ju YM, Takahashi H *et al.* Engineered small diameter vascular grafts by combining cell sheet engineering and electrospinning technology. *Acta Biomater.* 16, 14–22 (2015).

22 Flemming RG, Murphy CJ, Abrams GA, Goodman SL, Nealey PF. Effects of synthetic micro- and nano-structured surfaces on cell behavior. *Biomaterials* 20(6), 573–588 (1999).

23 Ju YM, Choi JS, Atala A, Yoo JJ, Lee SJ. Bilayered scaffold for engineering cellularized blood vessels. *Biomaterials* 31(15), 4313–4321 (2010).

24 Li WJ, Mauck RL, Cooper JA, Yuan X, Tuan RS. Engineering controllable anisotropy in electrospun biodegradable nanofibrous scaffolds for musculoskeletal tissue engineering. *J. Biomech.* 40(8), 1686–1693 (2007).

25 Zhang D, Chang J. Electrospinning of three-dimensional nanofibrous tubes with controllable architectures. *Nano Lett.* 8(10), 3283–3287 (2008).

26 Jayasinghe SN. Cell electrospinning: a novel tool for functionalising fibres, scaffolds and membranes with living cells and other advanced materials for regenerative biology and medicine. *Analyst* 138(8), 2215–2223 (2013).

27 Townsend-Nicholson A, Jayasinghe SN. Cell electrospinning: a unique biotechnique for encapsulating living organisms for generating active biological microthreads/scaffolds. *Biomacromolecules* 7(12), 3364–3369 (2006).

28 Yang D, Guo T, Nie C, Morris SF. Tissue-engineered blood vessel graft produced by self-derived cells and allogenic acellular matrix: a functional performance and histologic study. *Ann. Plast. Surg.* 62(3), 297–303 (2009).

29 Wang Y, Hu J, Jiao J *et al.* Engineering vascular tissue with functional smooth muscle cells derived from human iPS cells and nanofibrous scaffolds. *Biomaterials* 35(32), 8960–8969 (2014).

30 Xie C, Hu J, Ma H *et al.* Three-dimensional growth of iPS cell-derived smooth muscle cells on nanofibrous scaffolds. *Biomaterials* 32(19), 4369–4375 (2011).

31 Belair DG, Whisler JA, Valdez J *et al.* Human vascular tissue models formed from human induced pluripotent stem cell derived endothelial cells. *Stem Cell Rev.* 11(3), 511–525 (2014).

32 Gawaz M, Langer H, May AE. Platelets in inflammation and atherogenesis. *J. Clin. Invest.* 115(12), 3378–3384 (2005).

33 Huang NF, Okogbaa J, Lee JC *et al.* The modulation of endothelial cell morphology, function, and survival using anisotropic nanofibrillar collagen scaffolds. *Biomaterials* 34(16), 4038–4047 (2013).

•• **Describes the influence of aligned nanofibrillar scaffolds in modulating cell survival in an ischemic limb tissue.**

34 Dalby MJ, Gadegaard N, Oreffo RO. Harnessing nanotopography and integrin-matrix interactions to influence stem cell fate. *Nat. Mater.* 13(6), 558–569 (2014).

•• **Reviews the basic biology and mechanisms by which nanotopography influences cell function and stem cell fate.**

35 Chen W, Villa-Diaz LG, Sun Y *et al.* Nanotopography influences adhesion, spreading, and self-renewal of human embryonic stem cells. *ACS Nano* 6(5), 4094–4103 (2012).

36 Kong YP, Tu CH, Donovan PJ, Yee AF. Expression of oct4 in human embryonic stem cells is dependent on nanotopographical configuration. *Acta Biomater.* 9(5), 6369–6380 (2013).

37 Lin PH, Chen C, Bush RL, Yao Q, Lumsden AB, Hanson SR. Small-caliber heparin-coated ePTFE grafts reduce platelet deposition and neointimal hyperplasia in a baboon model. *J. Vasc. Surg.* 39(6), 1322–1328 (2004).

38 Hashi CK, Derugin N, Janairo RR *et al.* Antithrombogenic modification of small-diameter microfibrous vascular grafts. *Arterioscler. Thromb. Vasc. Biol.* 30(8), 1621–1627 (2010).

• **Utilizes aligned fibrillar vascular grafts to impart antithrombogenic property to vascular grafts.**

39 Nakayama KH, Hou L, Huang NF. Role of extracellular matrix signaling cues in modulating cell fate commitment for cardiovascular tissue engineering. *Adv. Healthc. Mater.* 3(5), 628–641 (2014).